SGLT1 is required for the survival of triple negative breast cancer cells via potentiating EGFR activity

Huiquan Liu[1], Ayse Ertay[2], Ping Peng[1], Juanjuan Li[2], Dian Liu[1], Hua Xiong[1], Yanmei Zou[1], Hong Qiu[1], David Hancock[4], Xianglin Yuan[1], Wei-Chien Huang[5,6,7], Rob M. Ewing[2,3], Julian Downward[4] and Yihua Wang[1,2,3]

1 Department of Oncology, Tongji Hospital, Tongji Medical College, Huazhong University of Science and Technology, Wuhan 430030, China.

2 Biological Sciences, Faculty of Environmental and Life Sciences, University of Southampton, Southampton SO17 1BJ, UK.

3 Institute for Life Sciences, University of Southampton, Southampton, SO17 1BJ, UK.

4 Oncogene Biology, The Francis Crick Institute, London NW1 1AT, UK.

5 Graduate Institute of Biomedical Sciences, China Medical University, Taichung 404, Taiwan.

6 Center for Molecular Medicine, China Medical University and Hospital, Taichung 404, Taiwan.

7 Department of Biotechnology, College of Health Science, Asia University, Taichung 413, Taiwan.

Correspondence

Y. Wang, Biological Sciences, Faculty of Environmental and Life Sciences, University of Southampton, Southampton SO17 1BJ, UK
E-mail: yihua.wang@soton.ac.uk

Keywords

SGLT1, triple negative breast cancer, EGFR

Abbreviation

TNBC, triple negative breast cancer; HER2, human epidermal growth factor 2; EGFR, epidermal growth factor receptor; SGLT1, sodium glucose cotransporter 1; ATCC, American Type Culture Collection; FBS, fetal bovine serum; shRNA, short hairpin RNA; siRNA, Short interfering RNA; MTT, 3-(4,5-Dimethyl-thiazol-2-yl)-2,5-diphenyltetrazolium bromide; IgG, immunoglobulin G; SPF, Specific pathogen-free; DAVID, Database for Annotation, Visualization and Integration Discovery; KEGG, Kyoto Encyclopedia of Genes and Genomes; PD-L1, programmed death-ligand 1.

Abstract

Sodium/glucose cotransporter 1 (SGLT1), an essential active glucose transport protein that helps maintain high intracellular glucose levels, was shown to interact with epidermal growth factor receptor (EGFR) and the SGLT1-EGFR interaction maintains the intracellular glucose level to promote survival of cancer cells. Here, we explore the role of SGLT1 in triple negative breast cancer (TNBC), which is the most aggressive type of breast cancer. We performed TCGA analysis coupled to *in vitro* experiments in TNBC cell lines as well as *in vivo* xenografts established in the mammary fat pad of female nude mice. Tissue microarrays of TNBC patients with information of clinic-pathological parameters were also used to investigate the expression and function of SGLT1 in TNBC. We show that high levels of SGLT1 are associated with greater tumour size in TNBC. Knockdown of SGLT1 compromises the cell growth *in vitro* and *in vivo*. We further demonstrate that SGLT1 depletion results in the decreased level of phospho-EGFR and as a result, the activity of downstream signalling pathways (such as AKT and ERK) is inhibited. Hence, targeting SGLT1 itself or EGFR-SGLT1 interaction may provide novel therapeutics against TNBC.

1. INTRODUCTION

Breast cancer is the most frequent cancer type in women with 1.38 million new cases (23%) each year throughout the world. It is the fifth leading cause of cancer death (458,000 deaths worldwide) and globally, the most frequent females cancer deaths in developing and developed countries (Ferlay *et al.*, 2010). Triple negative breast cancer (TNBC), which lacks expressions of oestrogen, progesterone and human epidermal growth factor 2 (HER2) receptors, accounts for 10-20% breast cancers with unsatisfactory therapeutic efficacy (O'Reilly *et al.*, 2015; Reis-Filho and Tutt, 2008). TNBC is the most aggressive, high-grade breast cancer type with high risk of metastasis and poor survival rate compared to the other breast cancer subtypes. Chemotherapy has been the only accepted systemic treatment option for TNBC for several years to increase the overall survival rate (Khosravi-Shahi *et al.*, 2018). However, drug resistance occurs due to its heterogeneity (Du *et al.*, 2015), and this contributes to the recurrence of the metastatic disease (Lee and Djamgoz, 2018). Therefore, it is crucial to identify targeted therapies for TNBC.

Novel targeted therapies, such as endocrine therapies and targeting HER2, were discovered by the mapping the genomic landscapes of breast cancer tumours. Genomic analysis has led to insights into the classification of TNBC such as the separation of TNBC into different subtypes based on gene expression (Criscitiello *et al.*, 2012; Garrido-Castro *et al.*, 2019; Network, 2012). However, due to its complexity and heterogeneity, it has been challenging to identify targeted therapies for TNBC (Lehmann *et al.*, 2011). Atezolizumab (TECENTRIQ®), an anti-programmed death-ligand 1 (PD-L1) monoclonal antibody, was approved recently as a first targeted therapy for TNBC with combination of chemotherapy (Abraxane; nab®-Paclitaxel) (Cyprian *et al.*, 2019). As atezolizumab plus chemotherapy combination is only successful for PD-L1 positive TNBC and TNBC is a heterogeneous

disease, further molecular studies are required to identify novel therapeutic targets for TNBC. Over the past decades, potential targeted therapies were discovered for TNBC by targeting different signalling pathways such as epidermal growth factor receptor (EGFR) (Crozier *et al.*, 2016; Nabholtz *et al.*, 2016; Schuler *et al.*, 2012; Shao *et al.*, 2017; Trédan *et al.*, 2015). However, targeting EGFR pathway was not very successful in part due to the resistance mechanisms or activation of different signalling pathway(s) (Baselga *et al.*, 2005; Baselga *et al.*, 2013; Carey *et al.*, 2012; Spector *et al.*, 2005). A previous study showed that inhibition of sodium/glucose cotransporter 1 (SGLT1) sensitised prostate cancer cells to EGFR inhibitors (Gefitinib and Erlotinib) (Wright *et al.*, 2011), although the precise mechanisms have not been elucidated. Knowing that SGLT1 mainly interacts with the auto-phosphorylation domain of EGFR (Ren *et al.*, 2013), we hypothesized that SGLT1 may regulate EGFR activity in TNBC.

SGLT1, encoded by the *SLC5A1* gene in human, is an active glucose transporter, which utilizes sodium gradients to transport glucose into cells independent of extracellular glucose concentration (Rieg and Vallon, 2018; Wright *et al.*, 2011). Various studies have discovered that SGLT1 is overexpressed in different cancer types; prostate cancer (Blessing *et al.*, 2012), ovarian carcinoma (Lai *et al.*, 2012), oral squamous cell carcinoma (Hanabata *et al.*, 2012), head and neck carcinoma (Wright *et al.*, 2011), pancreatic cancer (Casneuf *et al.*, 2008) and colorectal cancer (Guo *et al.*, 2011). In ovarian carcinoma, tumour development and poor prognosis of the disease is associated with overexpression of SGLT1 (Lai *et al.*, 2012). Overexpression of SGLT1 also has linked with higher clinical stages of colorectal cancer (Guo *et al.*, 2011). Despite of all these observations, the role of SGLT1 in TNBC was not known. In this study, we report that SGLT1 is essential for the survival of TNBC cells *in vitro* and *in vivo*. This is achieved, at least in part, via potentiating EGFR activity.

2. MATERIALS AND METHODS

2.1.Cell culture and transfection

BT549, MDA-MB-468 and MDA-MB-436 cell lines, which all belong to triple negative breast carcinoma cells, were purchased from Cell Bank of the Institute of Basic medicine, Chinese Academy of Medical Sciences (Beijing, China) or obtained as NCI-ICBP45 kit procured through American Type Culture Collection (ATCC) (ATCC Breast Cancer Cell Panel, Manassas, VA, USA). BT549 cells were cultured in RPMI 1640 medium (Boster, Wuhan, China) supplemented with 10% fetal bovine serum (FBS; Gibco, Carlsbad, USA), 1% antibiotics and 0.023IU/mL bovine insulin (Sigma-Aldrich, Saint Louis, USA). MDA-MB-436 and MDA-MB-468 cells were cultured in Dulbecco's Modified Eagle Medium (DMEM; Boster) with 20% or 10% FBS (Gibco) and 1% antibiotics. All cells were kept at 37°C and 5% CO2. The short hairpin RNA (shRNA) product of SGLT1 (sh-SGLT1) with a targeted sequence of ATCTTTCTCTTATTGGCAA and its negative control (sh-NC) were purchased from GeneChem (Shanghai, China) and transfected into cells according to manufacturer's instructions. Short interfering RNA (siRNA) oligos against SGLT1 (MU-007589-01-0002) was purchased from Dharmacon. Sequences are available from Dharmacon, or upon request. As a negative control, we used siGENOME RISC-Free siRNA (Dharmacon). Cells were transfected with the indicated siRNA oligos at a final concentration of 35 nM using Dharmafect 2 reagent (Dharmacon).

2.2. Cell viability assay

ShRNA transfected cells were seeded into 96-well plates with a density of 1×10^3 cells per well and allowed to grow for 24, 48 and 72 hours. When indicated time arrived, 3-(4,5-Dimethyl-thiazol-2-yl)-2,5-diphenyltetrazolium bromide (MTT) solution (Sangon Biotech,

Shanghai, China) was added into the medium with a final concentration of 0.5 mg/ml. The medium in each well was carefully sucked after incubation for 4 hours at 37°C and replaced by 100 μl formazan solubilization solution followed by gently mix for 10 minutes. OD values at 570nm were measured using Microplate Reader (Bioteck Instrument, Winooski, USA).

2.3.Western blot analysis

Western blot analysis was performed with lysates from cells or tissues with Urea buffer (8 M Urea, 1 M Thiourea, 0.5% CHAPS, 50 mM DTT, and 24 mM Spermine). For immunoprecipitations, the cells were lysed for 30 min at 4°C in pNAS buffer (50 mMTris-HCl [pH 7.5], 120 mM NaCl, 1 mM EDTA, and 0.1% Nonidet P-40), with protease inhibitors. Indicated antibodies and immunoglobulin G (IgG) agarose were added to the lysate for 16 hours at 4°C. Immunoprecipitates were washed four times with cold PBS followed by the addition of SDS sample buffer. The bound proteins were separated on SDS polyacrylamide gels and subjected to immunoblotting with the indicated antibodies. Primary antibodies were from: Abcam (SGLT1, 1:1000, ab14686; β-actin, 1:2000, ab8227; β-tubulin, 1:5000, ab6046; GAPDH, 1:2000, ab9385; Phospho-EGFR^{Tyr1068}, 1:1000, ab40815), Cell Signaling Technology (SGLT1, 1:1000, 5042; Phospho-EGFR^{Tyr1068}, 1:1000, 3777, D7A5; EGFR, 1:1000, 4267, D38B1; Phospho-AKT Ser473, 1:1000, 9271; Phospho-AKT Thr308, 1:1000, 4056, 244F9; AKT, 1:1000, 9272; Phospho-ERK (Thr202/Tyr204), 1:1000, 9101; ERK, 1:1000, 9102; Cleaved PARP Asp214, 1:1000, 9541), Millipore (PTEN, 1:1000, 04-409). Signals were detected using an ECL detection system (GE Healthcare) or an Odyssey imaging system (LI-COR), and evaluated by ImageJ 1.42q software (National Institutes of Health).

2.4.Immunofluorescence microscopy

Cells were fixed in 4% PBS-paraformaldehyde for 15 minutes, incubated in 0.1% Triton-X-100 for 5 minutes on ice, then in 0.2% Fish Skin Gelatine in PBS for 1 hour and stained for 1 hour with an anti-Phospho-EGFR^{Tyr1068} (1:100, Cell Signaling Technology, 3777). Protein expression was detected using Alexa Fluor (1:400, Molecular Probes) for 20 minutes. TO-PRO-3 (Invitrogen) was used to stain nucleic acids (1:2000).

2.5.Animal study

Animal experiments were carried out in accordance with the guidelines and approved protocols of the Ethics Committee of Tongji Hospital (Wuhan, China). Specific pathogen-free (SPF) nude mice (female, 6 weeks) were purchased from Vital River Laboratory Animal Technology Co., Ltd. (Beijing, China) and housed under specific pathogen free condition. After adaptation for one week in condition of stable temperature and humidity with 12 hours' light-dark cycle, mice were randomly divided into sh-NC group and sh-SGLT1 group (n = 6 mice per group). ShRNA transfected MDA-MB-436 cells were harvested, rinsed and resuspended in PBS at a concentration of 2×10^8 cells/ml, which were then placed on ice for subsequent operation. Orthotopic injection was performed in sterile condition in clean bench according to protocol described previously (Kocatürk and Versteeg, 2015) with adaptations. Briefly, after anesthetizing the mice intraperitoneally with sterilized 2% Avertin (Sigma-Aldrich) with a dosage of 0.12ml/10g weight, mammary gland was exposed by making a small incision between the fourth nipple and the midline. A total of 1×10^7 cells in 50 μl suspension were completely injected into mammary fat pad located in groin without leaking. Then the incisions were sutured and mice were attended until they gain consciousness. The lengths and widths of xenografts were measured weekly by vernier caliper and volume was calculated using following formula: V (mm^3) = 1/2*length*$widths^2$. At the end of

experiment, mice were sacrificed while xenografts were completely separated, measured and fixed by 4% paraformaldehyde for histological staining.

2.6.Immunohistochemical and H/E staining and scoring

Tissue microarray of triple negative breast cancer patients with information of clinic-pathological parameters was purchased from Outdo Biotech (HBreD090Bc01; Shanghai, China). Paraffin-embedded sections of xenograft tissues were subjected to deparaffinization and rehydration. H/E staining of sections was carried out using H/E staining kit (Beyotime, Shanghai, China) according to manufacturer's instructions. For immunohistochemical staining of tissue microarray and sections of xenograft, antigen retrieval, blocking of non-specific binding and incubation of primary antibodies at 4°C overnight was sequentially conducted. The primary antibodies used were list as follows: anti-phospho-EGFR (ab40815, Abcam, 1:200) and anti-SGLT1 (ab14686, Abcam, 1:100). After incubation with secondary goat anti-rabbit immunoglobulin conjugated to peroxidase-labeled dextran polymer (SV0002; Boster) at 37°C for 1 h, visualization, counterstaining with hematoxylin and mounting were performed. Semi-quantitative evaluations of protein expression were scored on the basis of the intensity and the percentage of phospho-EGFR or SGLT1 positive tumour cells as previously described (Wang *et al.*, 2014).

2.7.TCGA data mining and pathway analysis

SLC5A1, mRNA expression z-score (RNA Seq V2 RSEM) and molecular subtypes of breast invasive carcinoma (TCGA, Provisional) were obtained from cBioPortal for Cancer Genomics website (http://www.cbioportal.org/). Molecular subtypes of breast samples were

separated based on ER, PR and HER2 status and mRNA expression of SGLT1 was analysed in each subtype in GraphPad Prism 8 by ordinary one-way ANOVA.

Two different data sets, TCGA_BRCA_RPPA-2015-02-24 and TCGA_BRCA_exp_HiSeqV2-2015-02- 24, for RPPA protein expression and gene expression RNASeq (IlluminaHiSeq), respectively were extracted from UCSC Cancer Browser (https://genome-cancer.ucsc.edu/) for the analysis of genomic matrix data in TNBC samples. The data of TNBC samples that had SGLT1 mRNA expression from the cBioPortal for Cancer Genomics website was aligned with the samples in genomic matrix of TCGA data for both protein and gene expressions. For both protein and gene expression data sets, top 20% and bottom 20% of samples were chosen for high and low SGLT1 expression, respectively. Then, un-paired *t-test* was performed to find the significantly different proteins/genes between high and low SGLT1 groups in R version 3.4.4, $P < 0.05$. For the protein expression of AKT_pT308 in TCGA protein data set, prism8 was used to plot scatter dot plot between high and low SGLT1 groups.

To explore the pathway analysis of the TCGA gene data analysis, the Database for Annotation, Visualization and Integration Discovery (DAVID) functional annotation web tool was conducted (version 6.8; https://david.ncifcrf.gov/; (Huang *et al.*, 2009)). 1325 genes, which were positively correlated with SGLT1 in TCGA gene data, were analysed with DAVID web tool and obtained the lists of enriched Kyoto Encyclopedia of Genes and Genomes (KEGG) pathway, REACTOME pathway, BIOCARTA, BBID and EC number. A P value ≤ 0.05 was considered significant. The pathways were sorted from lowest p-value and top 34 pathways were chosen which then were sorted with highest number of shared genes. Subsequently, we then plotted that histogram plot with the top 15 pathways in GraphPad Prism 8.

2.8.Statistical analysis

Comparison of two groups was statistically calculated by student's *t*-test. Chi-square test was used to evaluate the relationship of SGLT1 expression and clinical parameters of triple negative breast cancer. Correlation between expressions of SGLT1 and phospho-EGFR was analyzed using Pearson's correlation. Data was shown as mean ± SD. Statistical analysis was conducted using SPSS version 19.0. Un-paired *t-test* was performed for TCGA data analysis in R version 3.4.4. To identify the statistical difference of AKT_pT308 between high and low SGLT1 group in TCGA protein data, un-paired *t-test* was performed in GraphPad Prism 8 software.

3. Results

3.1. SGLT1 expression is higher in TNBC, and this associates with a larger tumour size.

The expression of SGLT1 was up-regulated in various cancer types (Blessing *et al.*, 2012; Casneuf *et al.*, 2008; Guo *et al.*, 2011; Hanabata *et al.*, 2012; Lai *et al.*, 2012; Wright *et al.*, 2011). To investigate whether the expression of SGLT1 is different between each molecular subtype of breast cancer, TCGA breast invasive carcinoma (Provisional) data was analysed. The mRNA levels of SGLT1 (*SLC5A*) were significantly higher in TNBC and HER2-positive subtypes than luminal A and luminal B (Supplementary Fig. 1). No significant difference between TNBC and HER2-positive subtypes was observed (Supplementary Fig. 1).

In order to examine whether SGLT1 expression levels correlate with clinic-pathological features in TNBC, we performed immunohistochemistry (IHC) staining of SGLT1 in TNBC tissue microarrays. Table 1 shows clinical and pathological characteristics of the 90 TNBC patient samples. We found only tumour size was significantly affected by SGLT1 expression (Table 1). Representative images of high and low expression of SGLT1 in TNBC were shown in Fig. 1A. Tumour size was significantly larger in high SGLT1 TNBC samples compared to the low SGLT1 TNBC samples ($P = 0.006$; Fig. 1B).

3.2.SGLT1 depletion impairs cell viability of TNBC.

Given the fact that SGLT1 levels associate with tumour size, we next checked whether SGLT1 depletion impairs cell viability. MTT assay was performed in control or SGLT1-depleted MDA-MB-436, MDA-MB-468 and BT549 cell lines (Supplementary Fig. 2). The OD values in MDA-MB-436, MDA-MB-468 and BT549 cells was significantly decreased in SGLT1-depleted ones compared to the controls in various time points (Fig. 2A). We subsequently performed an *in vivo* study to determine the effect of SGLT1 knockdown on

tumour growth. MDA-MB-436 tumours were established in the mammary fat pad of female nude mice. As shown in Fig. 2B, tumours were found in 4 of 6 mice where control MDA-MB-436 cells were injected, whereas only 2 of 6 mice had tumours where SGLT1-depleted MDA-MB-436 cells were injected. The volume and weight of tumours present in the mice injected with SGLT1-depleted MDA-MB-436 cells were significantly lower than that in the control group injected with control cells (Fig. 2B). Hence, a reduction in SGLT1 expression is able to inhibit TNBC cell growth *in vitro* and *in vivo*.

3.3. TCGA analysis reveals a link between SGLT1 status and AKT signalling in TNBC samples.

In order to find how SGLT1 regulates tumour growth, we analysed data from the TCGA project. Protein (RPPA) TCGA breast invasive carcinoma data and Gene, RNASeq (IlluminaHiSeq) TCGA breast invasive carcinoma data sets were obtained from UCSC Cancer Genomics Browser (https://genome-cancer.ucsc.edu/). Protein expression data included 410 breast invasive carcinoma samples and 142 proteins; and gene expression data contained 1215 samples and 20530 genes. Both protein (RPPA) and gene expression, RNASeq (IlluminaHiSeq) breast invasive carcinoma samples from Cancer Genome Browser were aligned with TNBC samples, as shown in Supplementary Fig. 1. The alignment showed 59 and 160 TNBC samples in protein (RPPA) and gene, RNASeq (IlluminaHiSeq) data, respectively. In both protein and gene expression data sets, the top 20% and bottom 20% samples were separated into two groups; high and low SGLT1 expressing samples, respectively and un-paired *t*-test was performed to find the significantly different proteins/genes between the groups. A heat-map of protein expression for 19 proteins, including phosphorylated AKT (AKT_pT308), that were significantly different between high and low SGLT1 expressing samples ($P < 0.05$) is shown in Fig. 3A. The scatter dot plot

showed the protein expression of phosphorylated AKT (AKT_pT308) for each sample in high and low SGLT1 groups (Fig. 3B). 2279 significantly different genes between high and low SGLT1 expressing samples are shown by the heat-map (Fig. 3C).

To demonstrate whether the significantly positive genes with SGLT1 in TCGA data set are involved in the same pathway, DAVID, online website (https://david.ncifcrf.gov/) was used to perform a pathway analysis. We found PI3K-AKT signalling pathway is the top pathway that has the highest hit genes, followed by Ras signalling and other pathways (Fig. 3D). These analyses suggested that SGLT1 may interact with AKT signalling pathway.

3.4.SGLT1 binds EGFR and positively regulates EGFR activity.

STRING (Search Tool for the Retrieval of Interacting Genes) (https://string-db.org/) analysis showed the interaction between SGLT1 and EGFR (Supplementary Fig. 3), which was reported earlier (Ren *et al.*, 2013; Weihua *et al.*, 2008). In fact, we also observed EGFR-SGLT1 interaction in MDA-MB-468 human breast cancer cells. Endogenous EGFR and SGLT1 co-immunoprecipitated together in MDA-MB-468 cells (Fig. 4A).

Given that SGLT1 interacts primarily with the auto-phosphorylation domain of EGFR (Ren *et al.*, 2013), we asked whether SGLT1 status could also affect EGFR activity on the other hand. Consistently, the immunofluorescence signal of phospho-EGFR^{Tyr1068} was at the cell membrane in MDA-MB-468 cells (Fig. 4B). To test the biological importance of the observed EGFR-SGLT1 interaction, we examined the level of phospho-EGFR^{Tyr1068} by immunofluorescence staining in MDA-MB-468 cells treated with control small interfering RNA (siRNA) or siRNA against SGLT1. Importantly, SGLT1 depletion by RNA interference (RNAi) largely abolished the membrane signal of phospho-EGFR^{Tyr1068} (Fig. 4B). For most of the analyses described here we used pools of four siRNAs against each gene ("SMARTpools" from Dharmacon). However, deconvolution of siRNA pools into their

constituent individual oligonucleotides is an important step in minimizing the potential for off-target effects to compromise the analysis of gene knockdown studies (Echeverri *et al.*, 2006). Supplementary Fig. 4 showed that deconvolution of SGLT1 siRNA SMARTpool, two out of four different oligonucleotides, clearly led to the down-regulation of SGLT1 and reduced level of phospho-EGFR^{Tyr1068}.

We next asked whether SGLT1 status could affect the activity of EGFR downstream pathways, which was investigated by examining the EGFR signalling cascade in MDA-MB-468 cells transfected with control siRNA or SGLT1 siRNA. The basal phosphorylation levels of EGFR (Tyr1068) and AKT (Ser473 and Thr308) was reduced in SGLT1-depleted MDA-MB-468 cells compared to control cells or control siRNA-treated cells. Total protein levels of EGFR and AKT, however, were not affected (Fig. 4C). Following SGLT1 gene silencing in MDA-MB-468 cells, a rapid and profound loss of cell viability was observed, most likely resulting from a robust induction of apoptosis. This is evident by the detection of poly ADP ribose polymerase (PARP) cleavage, a well-described indicator of effector caspase activation and consequent cell death (Fig. 4C).

The difference was more notable upon EGF treatment. A much stronger response induced by addition of EGF was observed in control siRNA-treated cells compared with SGLT1-depleted MDA-MB-468 cells, reflected by the phosphorylation levels of EGFR (Tyr1068), ERK (Thr202/Tyr204) and AKT (Ser473) (Fig. 4D). These data suggest that by binding to EGFR, SGLT1 potentiates EGFR signalling.

To further validate the *in vitro* findings, the regulation of EGFR phosphorylation by SGLT1 was investigated *in vivo* using tumour sections derived from control shRNA or SGLT1 shRNA transfected MDA-MB-436 cells (Fig. 2B). Using adjacent tumour sections derived from MDA-MB-436–control shRNA cells, we observed positive SGLT1 and EGFR

phosphorylation. In tumours derived from MDA-MB-436–SGLT1 shRNA cells, SGLT1 negative tumour regions showed reduced levels of EGFR phosphorylation (Fig. 5). In addition, the correlation of SGLT1 expression and EGFR phosphorylation levels were analysed in TNBC samples (Fig. 6). High SGLT1 correlated with high EGFR phosphorylation levels in TNBC ($P < 0.0001$). These observations agree with the finding that SGLT1 potentiates EGFR signalling in TNBC.

4. Discussion

Chemotherapy has been the only systemic treatment option for TNBCs for several years to increase the overall survival rate of the patients (Khosravi-Shahi *et al.*, 2018), but chemotherapy-resistance is the major challenge for treatment of the patients with TNBC (Lee and Djamgoz, 2018). Therefore, several studies detected the molecular changes before and after the chemotherapy to identify potential targeted therapy for TNBC (Balko *et al.*, 2014). Identification of targeted therapy for the patients with TNBC could help to prevent the risk of resistance of the treatment option and recurrence of the disease. In this study, we showed that targeting of SGLT1 has the potential to treat TNBC. We found SGLT1 status associates with tumour size in TNBC. Similarly, SGLT1 expression showed significant association with clinic-pathological characteristics and prognosis of ovarian cancer; SGLT1 overexpression significantly correlated with increased pT status and poor prognosis (Lai *et al.*, 2012). Guo *et al.* 2011 also reported that higher expression of SGLT1 significantly associated with the clinical stage of colorectal cancer (Guo *et al.*, 2011).

SGLT1 is an active glucose transporter and plays a critical role in glucose absorption and retention in the body (Wright *et al.*, 2011). In cancer cells, a high rate of glucose uptake is required to meet the increased energy needs and leads to abnormal growth of cancerous cells (Hanahan and Weinberg, 2011). Depletion or inhibition of SGLT1 may reduce the energy supply to the cancer cells. In addition, we demonstrated that down-regulation of SGLT1 dampened EGFR-AKT or -ERK pathways activity, which phosphorylates a plethora of targets to activate the cell cycle, prevent apoptosis and trigger cellular growth (Downward, 2003; Manning and Cantley, 2007). As a result, SGLT1 depletion induced apoptosis in TNBC cells, and inhibited their growth *in vitro* and *in vivo*. Consistently, over-expression of SGLT1 protected renal epithelial cells (Ikari *et al.*, 2005) and intestinal epithelial cells (Yu *et al.*, 2008) from apoptosis.

Upon activation by its growth factor ligands, EGFR undergoes a transition from an inactive monomeric form to an active homodimer (Yarden and Schlessinger, 1987). EGFR dimerization stimulates its intrinsic intracellular protein-tyrosine kinase activity. As a result, auto-phosphorylation of several tyrosine residues in the C-terminal domain of EGFR occurs (Downward *et al.*, 1984; Lemmon *et al.*, 2014). This auto-phosphorylation elicits downstream activation and signalling. For example, growth factor receptor-bound protein 2 (GRB2) binds activated EGFR at phospho-Tyr1068, which is crucial to the EGF-induced activation of Ras signalling pathway (Rojas *et al.*, 1996). It was demonstrated auto-phosphorylation of EGFR is taking place primarily by activated EGFR located at the cell membrane (Sousa *et al.*, 2012). Down-regulation of SGLT1 by RNAi resulted in the decreased level of phospho-$EGFR^{Tyr1068}$ and as a result, the activity of downstream signalling pathways (such as AKT and ERK) was inhibited, suggesting that SGLT1 may facilitate the auto-phosphorylation of EGFR upon ligand binding. This result was also supported by significantly positive correlation between phospho-EGFR and SGLT1 in TNBC samples.

In line with the previous report indicating that loss of EGFR protein but not its tyrosine kinase activity sensitized cancer cells to chemotherapeutic agent (Weihua *et al.*, 2008), EGFR tyrosine kinase inhibitors did not produce therapeutic effects for certain cancers (Cohen *et al.*, 2003; Dancey and Freidlin, 2003; Fukuoka *et al.*, 2003). It has been highlighted EGFR tyrosine kinase inhibitors or monoclonal antibodies against TNBC showed low response rate, and the combination treatment with tyrosine kinase inhibitors or monoclonal antibodies and chemotherapy also showed low response rate and no benefits in the survival rate of patients (Baselga *et al.*, 2013; Carey *et al.*, 2012; Finn *et al.*, 2009; Lee and Djamgoz, 2018; Schuler *et al.*, 2010). Therefore, further works are needed to find out the best way to use EGFR targeted therapy in TNBC. EGFR–SGLT1 interaction stabilizes SGLT1 for the high uptake of glucose by cancerous cells and leads to the progression of cancer (Ren *et al.*, 2013;

Weihua *et al.*, 2008). EGFR depletion (Weihua *et al.*, 2008) or deletion of the SGLT1 interacting domain in EGFR promoted the down-regulation of SGTL1 via the proteasome machinery (Ren *et al.*, 2013). Together, targeting SGLT1 itself or EGFR-SGLT1 interaction might potentially provide novel therapeutics for TNBC patients.

Acknowledgements

This project was supported by the Ministry of Science and Technology of China National Key Research and Development Projects [2016YFC0904701], the National Natural Science Foundation of China [81772827], the Academy of Medical Sciences/the Wellcome Trust Springboard Award [SBF002\1038] and the Wessex Medical Trust. HL was grateful for the scholarship provided by the Whale Education Foundation (Shenzhen, China). AE was supported by the Wessex Medical Trust. YZ was supported by the Natural Science Foundation of Hubei Province [No. 2018CFB611]. WC was supported by China Medical University Hospital [DMR-108-100]. JD was supported by the Francis Crick Institute which receives its core funding from Cancer Research UK (FC001070), the UK Medical Research Council (FC001070), and the Wellcome Trust (FC001070).

Conflict of interest

The authors declare no conflict of interest.

Author contributions

HL, AE, PP contributed equally in this work.

References

Balko JM, Giltnane JM, Wang K, Schwarz LJ, Young CD, Cook RS, … Arteaga CL (2014) Molecular profiling of the residual disease of triple-negative breast cancers after neoadjuvant chemotherapy identifies actionable therapeutic targets *Cancer Discov* **4**, 232–245.

Baselga J, Albanell J, Ruiz A, Lluch A, Gasco´n P, Guille´m V, … Federico R (2005) Phase II and Tumor Pharmacodynamic Study of Gefitinib in Patients with Advanced Breast Cancer *J Clin Oncol* **23**, 5323–5333.

Baselga J, Gómez P, Greil R, Braga S, Climent MA, Wardley AM, … Awada A (2013) Randomized phase II study of the anti-epidermal growth factor receptor monoclonal antibody cetuximab with cisplatin versus cisplatin alone in patients with metastatic triple-negative breast cancer *J Clin Oncol* **31**, 2586–2592.

Blessing A, Xu L, Gao G, Bollu LR, Ren J, Li H, … Huang W (2012) Sodium / Glucose Co-transporter 1 Expression Increases in Human Diseased Prostate *J Cancer Sci Ther* **4**, 306–312.

Carey LA, Rugo HS, Marcom PK, Mayer EL, Esteva FJ, Ma CX, … Winer EP (2012) TBCRC 001: Randomized phase II study of cetuximab in combination with carboplatin in stage IV triple-negative breast cancer *J Clin Oncol* **30**, 2615–2623.

Casneuf VF, Fonteyne P, Van Damme N, Demetter P, Pauwels P, De Hemptinne B, … Peeters M (2008) Expression of SGLT1, Bcl-2 and p53 in primary pancreatic cancer related to survival *Cancer Invest* **26**, 852–859.

Cohen EEW, Rosen F, Stadler WM, Recant W, Stenson K, Huo D, and Vokes EE (2003) Phase II trial of ZD1839 in recurrent or metastatic squamous cell carcinoma of the head and neck *J Clin Oncol* **21**, 1980–1987.

Criscitiello C, Azim HA, Schouten PC, Linn SC, and Sotiriou C (2012) Understanding the biology of triple-negative breast cancer *Ann Oncol* **23**.

Crozier JA, Advani PP, LaPlant B, Hobday T, Jaslowski AJ, Moreno-Aspita A, and Perez EA (2016) N0436 (Alliance): A phase II trial of irinotecan plus cetuximab in patients with metastatic breast cancer previously exposed to anthracycline and/or taxane-containing therapy *Clin Breast Cancer* **16**, 23–30.

Cyprian FS, Akhtar S, Gatalica Z, and Vranic S (2019) Targeted immunotherapy with a checkpoint inhibitor in combination with chemotherapy: A new clinical paradigm in the treatment of triple-negative breast cancer *Bosn J Basic Med Sci* 1–7.

Dancey JE, and Freidlin B (2003) Targeting epidermal growth factor receptor - Are we missing the mark? *Lancet* **362**, 62–64.

Downward J (2003) Targeting RAS signalling pathways in cancer therapy *Nat Rev Cancer* **3**, 11–22.

Downward J, Parker P, and Waterfield M (1984) Autophosphorylation sites on the epidermal growth factor receptor *Nature* **311**, 483–485.

Du F Le, Eckhardt BL, Lim B, Litton JK, Moulder S, Meric-Bernstam F, … Ueno NT (2015) Is the future of personalized therapy in triple-negative breast cancer based on molecular

subtype? *Oncotarget* **6**, 12890–12908.

Echeverri CJ, Beachy PA, Baum B, Boutros M, Buchholz F, Chanda SK, … Bernards R (2006) Minimizing the risk of reporting false positives in large-scale RNAi screens *Nat Methods* **3**, 777–779.

Ferlay J, Shin HR, Bray F, Forman D, Mathers C, and Parkin DM (2010) Estimates of worldwide burden of cancer in 2008: GLOBOCAN 2008 *Int J Cancer* **127**, 2893–2917.

Finn RS, Press MF, Dering J, Arbushites M, Koehler M, Oliva C, … Di Leo A (2009) Estrogen receptor, progesterone receptor, human epidermal growth factor receptor 2 (HER2), and epidermal growth factor receptor expression and benefit from lapatinib in a randomized trial of paclitaxel with lapatinib or placebo as first-line treatment in HER2-negative or unknown metastatic breast cancer *J Clin Oncol* **27**, 3908–3915.

Fukuoka M, Yano S, Giaccone G, Tamura T, Nakagawa K, Douillard JY, … Baselga J (2003) Multi-institutional randomized phase II trial of gefitinib for previously treated patients with advanced non-small-cell lung cancer *J Clin Oncol* **21**, 2237–2246.

Garrido-Castro AC, Lin NU, and Polyak K (2019) Insights into Molecular Classifications of Triple-Negative Breast Cancer: Improving Patient Selection for Treatment *Cancer Discov* 617–632.

Guo GF, Cai YC, Zhang B, Xu RH, Qiu HJ, Xia LP, … Wang F (2011) Overexpression of SGLT1 and EGFR in colorectal cancer showing a correlation with the prognosis *Med Oncol* **28**, S197–S203.

Hanabata Y, Nakajima Y, Morita K ichi, Kayamori K, and Omura K (2012) Coexpression of SGLT1 and EGFR is associated with tumor differentiation in oral squamous cell carcinoma *Odontology* **100**, 156–163.

Hanahan D, and Weinberg RA (2011) Hallmarks of cancer: The next generation *Cell* **144**, 646–674.

Huang DW, Sherman BT, and Lempicki RA (2009) Systematic and integrative analysis of large gene lists using DAVID bioinformatics resources *Nat Protoc* **4**, 44–57.

Ikari A, Nagatani Y, Tsukimoto M, Harada H, Miwa M, and Takagi K (2005) Sodium-dependent glucose transporter reduces peroxynitrite and cell injury caused by cisplatin in renal tubular epithelial cells *Biochim Biophys Acta - Biomembr* **1717**, 109–117.

Khosravi-Shahi P, Cabezón-Gutiérrez L, and Custodio-Cabello S (2018) Metastatic triple negative breast cancer: Optimizing treatment options, new and emerging targeted therapies *Asia Pac J Clin Oncol* **14**, 32–39.

Kocatürk B, and Versteeg HH (2015) Orthotopic Injection of Breast Cancer Cells into the Mammary Fat Pad of Mice to Study Tumor Growth. *J Vis Exp* 1–8.

Lai B, Xiao Y, Pu H, Cao Q, Jing H, and Liu X (2012) Overexpression of SGLT1 is correlated with tumor development and poor prognosis of ovarian carcinoma *Arch Gynecol Obstet* **285**, 1455–1461.

Lee A, and Djamgoz MBA (2018) Triple negative breast cancer: Emerging therapeutic modalities and novel combination therapies *Cancer Treat Rev* **62**, 110–122.

Lehmann BDB, Bauer J a J, Chen X, Sanders ME, Chakravarthy a B, Shyr Y, and Pietenpol

J a (2011) Identification of human triple-negative breast cancer subtypes and preclinical models for selection of targeted therapies *J Clin Invest* **121**, 2750–2767.

Lemmon MA, Schlessinger J, and Ferguson KM (2014) The EGFR Family: Not So Prototypical Receptor Tyrosine Kinases *Cold Spring Harb Perspect Biol* **6**, a020768.

Manning BD, and Cantley LC (2007) AKT/PKB Signaling: Navigating Downstream *Cell* **129**, 1261–1274.

Nabholtz JM, Chalabi N, Radosevic-Robin N, Dauplat MM, Mouret-Reynier MA, Van Praagh I, … Penault-Llorca F (2016) Multicentric neoadjuvant pilot Phase II study of cetuximab combined with docetaxel in operable triple negative breast cancer *Int J Cancer* **138**, 2274–2280.

Network TCGA (2012) Comprehensive molecular portraits of human breast tumors *Nature* **490**, 61–70.

O'Reilly EA, Gubbins L, Sharma S, Tully R, Guang MHZ, Weiner-Gorzel K, … McCann A (2015) The fate of chemoresistance in triple negative breast cancer (TNBC) *BBA Clin* **3**, 257–275.

Reis-Filho JS, and Tutt ANJ (2008) Triple negative tumours: A critical review *Histopathology* **52**, 108–118.

Ren J, Bollu LR, Su F, Gao G, Xu L, Huang WC, … Weihua Z (2013) EGFR-SGLT1 interaction does not respond to EGFR modulators, but inhibition of SGLT1 sensitizes prostate cancer cells to EGFR tyrosine kinase inhibitors *Prostate* **73**, 1453–1461.

Rieg T, and Vallon V (2018) Development of SGLT1 and SGLT2 inhibitors *Diabetologia* **61**, 2079–2086.

Rojas M, Yao S, and Lin YZ (1996) Controlling Epidermal Growth Factor (EGF)-stimulated Ras Activation in Intact Cells by a Cell-permeable Peptide Mimicking Phosphorylated EGF Receptor *J Biol Chem* **271**, 27456–27461.

Schuler M, Awada A, Harter P, Canon JL, Possinger K, Schmidt M, … Harbeck N (2012) A phase II trial to assess efficacy and safety of afatinib in extensively pretreated patients with HER2-negative metastatic breast cancer *Breast Cancer Res Treat* **134**, 1149–1159.

Schuler MH, Uttenreuther-Fisher MM, Piccart-Gebhart MJ, and Harbeck N (2010) BIBW 2992, a novel irreversible EGFR/HER1 and HER2 tyrosine kinase inhibitor, for the treatment of patients with HER2-negative metastatic breast cancer after failure of no more than two prior chemotherapies *J Clin Oncol* **28**, 1065–1065.

Shao F, Sun H, and Deng C-X (2017) Potential therapeutic targets of triple-negative breast cancer based on its intrinsic subtype *Oncotarget* **8**, 73329–73344.

Sousa LP, Lax I, Shen H, Ferguson SM, Camilli PD, and Schlessinger J (2012) Suppression of EGFR endocytosis by dynamin depletion reveals that EGFR signaling occurs primarily at the plasma membrane *Proc Natl Acad Sci* **109**, 4419–4424.

Spector NL, Xia W, Burris H, Hurwitz H, Dees EC, Dowlati A, … Bacus S (2005) Study of the biologic effects of lapatinib, a reversible inhibitor of ErbB1 and ErbB2 tyrosine kinases, on tumor growth and survival pathways in patients with advanced malignancies *J Clin Oncol* **23**, 2502–2512.

Trédan O, Campone M, Jassem J, Vyzula R, Coudert B, Pacilio C, … Roché H (2015) Ixabepilone alone or with cetuximab as first-line treatment for advanced/metastatic triple-negative breast cancer *Clin Breast Cancer* **15**, 8–15.

Wang Y, Bu F, Royer C, Serres S, Larkin JR, Soto MS, … Lu X (2014) ASPP2 controls epithelial plasticity and inhibits metastasis through β 2-catenin-dependent regulation of ZEB1 *Nat Cell Biol* **16**, 1092–1104.

Weihua Z, Tsan R, Huang WC, Wu Q, Chiu CH, Fidler IJ, and Hung MC (2008) Survival of Cancer Cells Is Maintained by EGFR Independent of Its Kinase Activity *Cancer Cell* **13**, 385–393.

Wright E, Loo D, and Hirayama B (2011) Biology of Human Sodium Glucose Transporters *Physiol Rev* **91**, 733–794.

Yarden Y, and Schlessinger J (1987) Epidermal Growth Factor Induces Rapid, Reversible Aggregation of the Purified Epidermal Growth Factor Receptor *Biochemistry* **26**, 1443–1451.

Yu LCH, Huang C ying, Kuo W ting, Sayer H, Turner JR, and Buret AG (2008) SGLT-1-mediated glucose uptake protects human intestinal epithelial cells against Giardia duodenalis-induced apoptosis *Int J Parasitol* **38**, 923–934.

Figure Legends

Figure 1. SGLT1 expression levels associate with tumour size in triple negative breast carcinoma (TNBC).

A) Representative SGLT1 staining pattern (High or Low SGLT1) in 90 TNBC tissue microarray cores. Scale bar: 100 μm. **B**) The relationship between SGLT1 expression and tumour size in TNBC samples was analysed ($P = 0.006$).

Figure 2. SGLT1 depletion impairs cell viability of TNBC *in vitro* and *in vivo*.

A) Knockdown of SGLT1 in BT549, MDA-MB-436 and MDA-MB-468 cells resulted in cell growth inhibition as performed by MTT assay. Data are represented as a mean value ± standard deviation of three independent experiments. * $P < 0.05$; ** $P < 0.01$ and *** $P < 0.001$. **B**) Graphs showing tumour volume ($P = 0.04$) or weight ($P = 0.03$) present in the mice injected with control or SGLT1-depleted MDA-MB-436 cells. Pictures of the tumours formed were also shown. Scale bar: 1 cm.

Figure 3. TCGA analysis reveals a link between SGLT1 status and AKT signalling in TNBC samples.

Heat-maps of the columns indicate each individual sample in high and low SGLT1 groups across each protein (**A**) and gene (**C**) in TCGA breast invasive carcinoma data, which obtained from Cancer Genome Browser. Rows indicates protein expressions (RPPA) (**A**) and gene expressions (IlluminaHiSeq) (**C**). Dark blue colour indicates low expression of proteins/genes and dark pink colour illustrates highly expressed proteins/genes. Unpaired *t*-test was analysed to find the significantly different proteins/genes in TCGA breast invasive

carcinoma data sets. *n* represents the number of samples in each group. **B**) Box plot shows the protein expression of AKT_pT308 between high and low SGLT1 groups in TNBC, TCGA breast invasive carcinoma. **P* < 0.05. **D**) The genes that were positively regulated with SGLT1 was analysed in DAVID website to show which pathways are regulated. Histogram shows top 15 pathways based on lowest p-value. Y-axis shows the pathways and top x-axis and bottom x-axis show the number of shared genes in each pathway and -log10 (*P* value), respectively.

Figure 4. SGLT1 binds EGFR and positively regulates EGFR activity.

A) Total cell lysates from MDA-MB-468 cells were immunoprecipitated with an anti-EGFR antibody or control IgG. EGFR and SGLT1 levels are indicated. IgG_H indicates IgG heavy chain. **B**) Immunofluorescence staining of Phospho-$EGFR^{Tyr1068}$ (green) in MDA-MB-468 cells transfected with SGLT1 siRNA or control siRNA. TO-PRO-3 (blue) was used to stain nuclei. Scale bar: 10 μm. **C**) Protein expression of Phospho-$EGFR^{Tyr1068}$, EGFR, Phospho-AKT Ser473, Phospho-AKT Ser308, AKT, Cleaved PARP Asp214 and SGLT1 in MDA-MB-468 cells with indicated treatments. β-tubulin was used as a loading control. **D**) Protein expression of Phospho-$EGFR^{Tyr1068}$, EGFR, Phospho-AKT Ser473, Phospho-ERK (Thr202/Tyr204) and SGLT1 in MDA-MB-468 cells with indicated treatments. β-tubulin was used as a loading control.

Figure 5. Down-regulation of SGLT1 reduces EGFR phosphorylation level *in vivo*. Adjacent tumour sections from representative cases of tumour xenografts formed by MDA-MB-436 cells treated with control or SGLT1 shRNA were stained with H/E. The expression of SGLT1 and p-EGFR are also indicated. Scale bars: 100 μm.

Figure 6. SGLT1 expression levels positively correlate with EGFR phosphorylation in TNBC.

A) Adjacent tumour sections from representative cases show SGLT1 and p-EGFR expression in TNBC. Scale bar: 100 μm. **B**) The relationship between SGLT1 expression and EGFR phosphorylation was analyzed by Pearson correlation test (R = 0.41, n = 90, $P < 0.0001$).

Table 1. The relationship between patients' clinic-pathological characteristics and SGLT1 expression in TNBC.

Figure 1

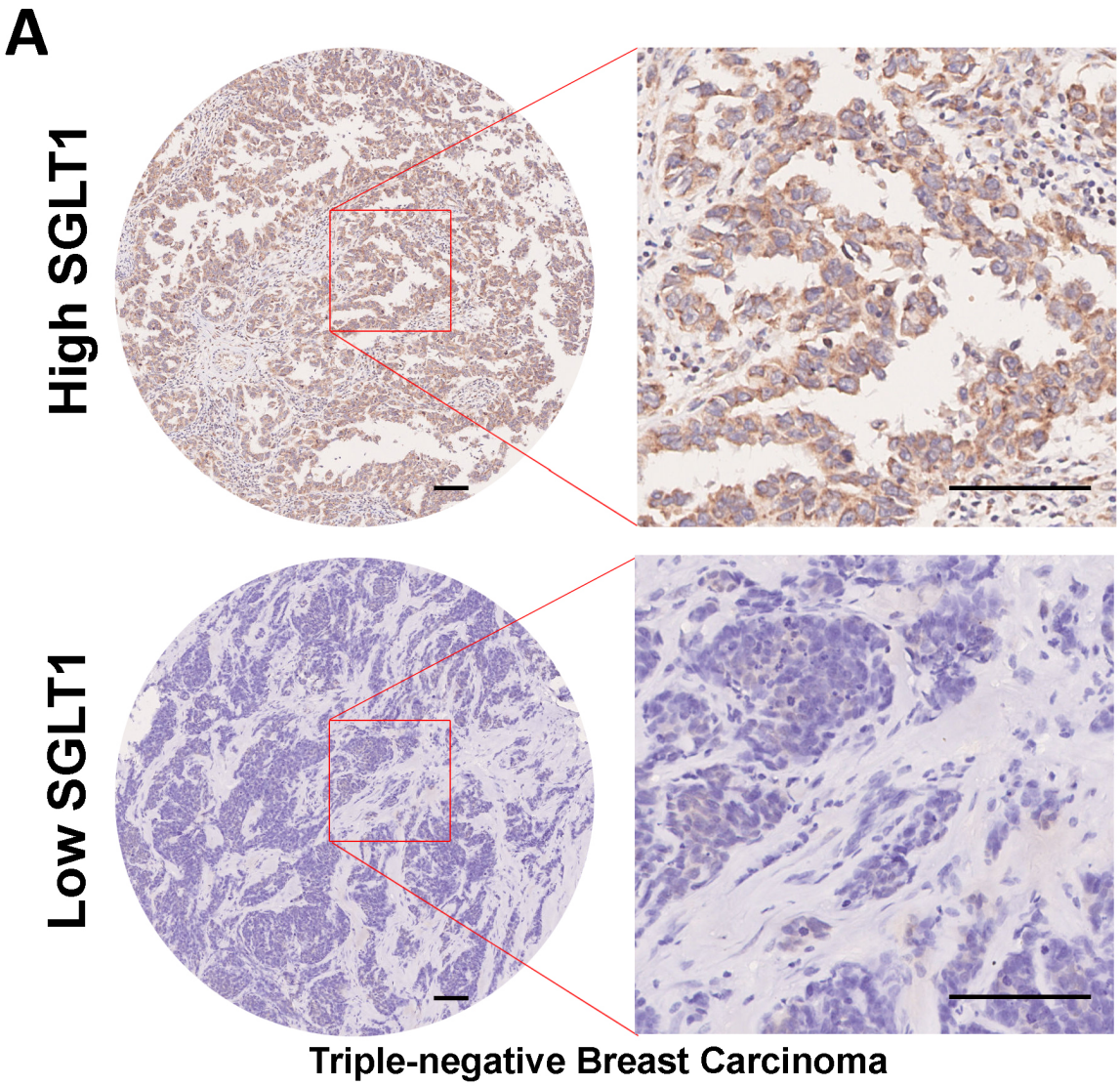
A
High SGLT1
Low SGLT1
Triple-negative Breast Carcinoma
B
P = 0.006
Tumour Size (cm)
0
2
4
6
8
10
Low SGLT1
High SGLT1

Figure 2

A

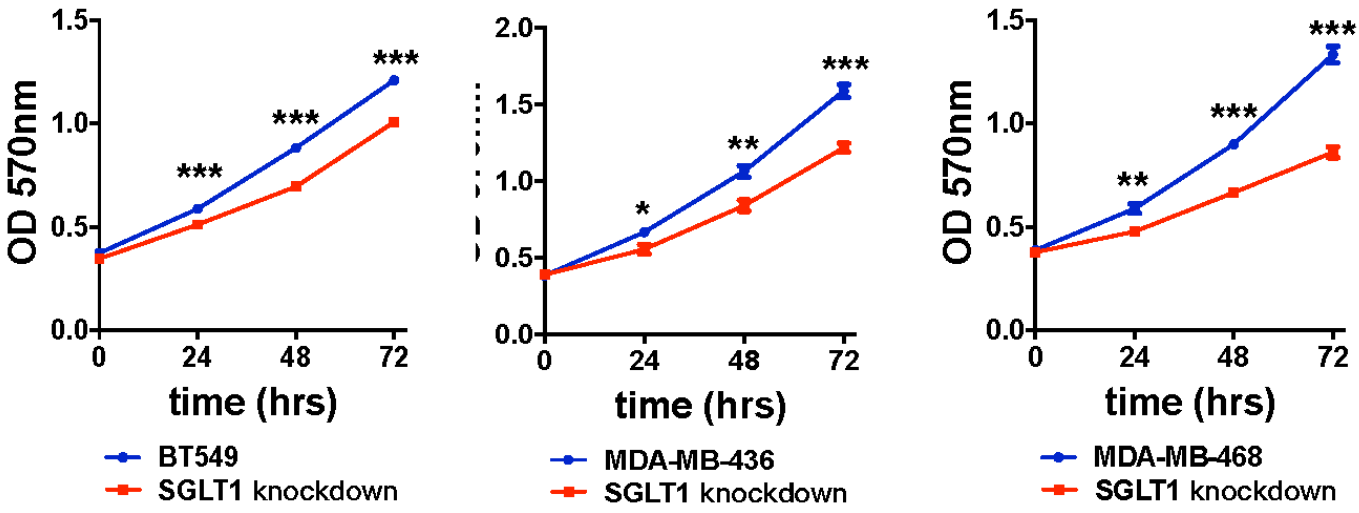
OD 570nm
time (hrs)
BT549
SGLT1 knockdown
MDA-MB-436
SGLT1 knockdown
MDA-MB-468
SGLT1 knockdown

B

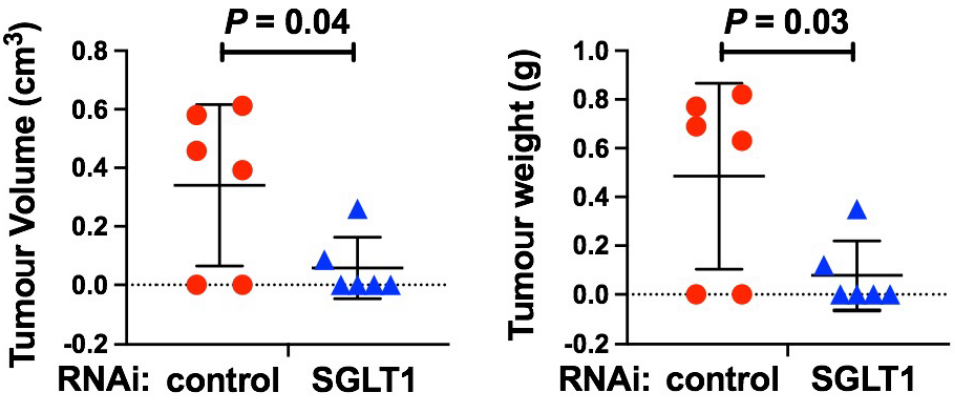
P = 0.04
Tumour Volume (cm3)
RNAi: control
SGLT1
P = 0.03
Tumour weight (g)
RNAi: control
SGLT1

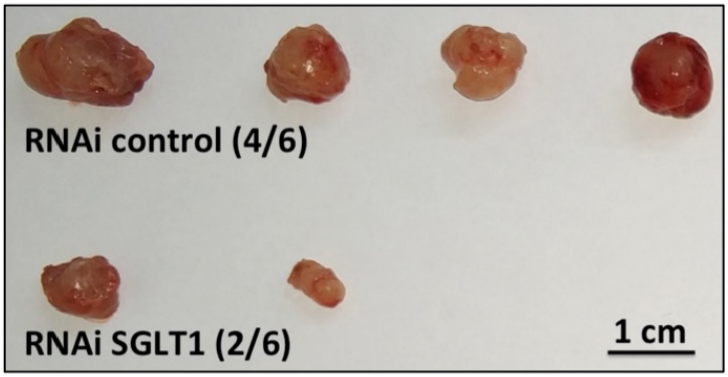
RNAi control (4/6)
RNAi SGLT1 (2/6)
1 cm

Figure 3

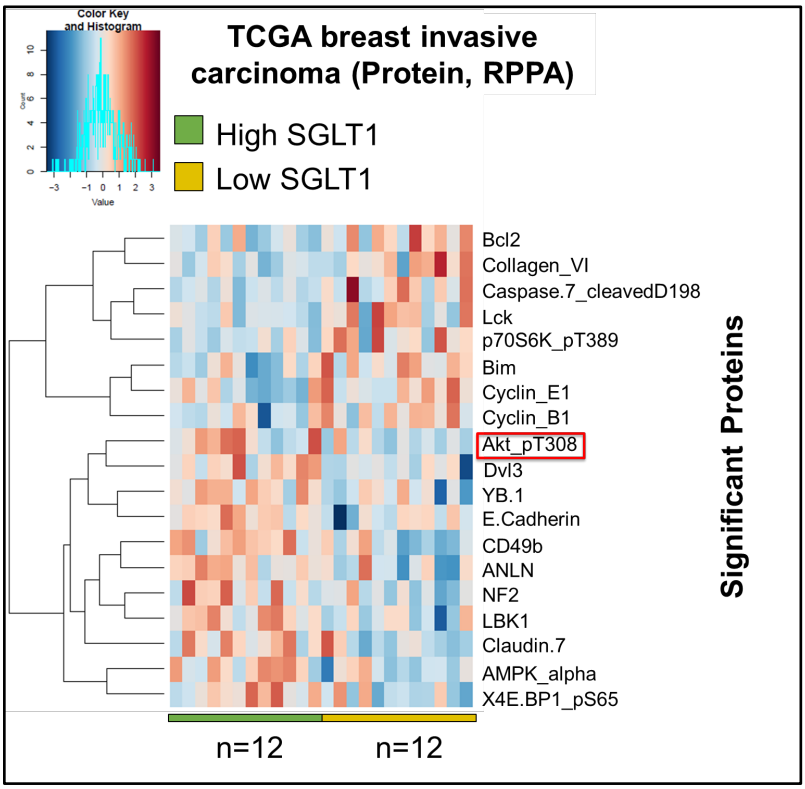
A
Color Key and Histogram
TCGA breast invasive carcinoma (Protein, RPPA)
High SGLT1
Low SGLT1
Bcl2
Collagen_VI
Caspase.7_cleavedD198
Lck
p70S6K_pT389
Bim
Cyclin_E1
Cyclin_B1
Akt_pT308
Dvl3
YB.1
E.Cadherin
CD49b
ANLN
NF2
LBK1
Claudin.7
AMPK_alpha
X4E.BP1_pS65
Significant Proteins
n=12
n=12

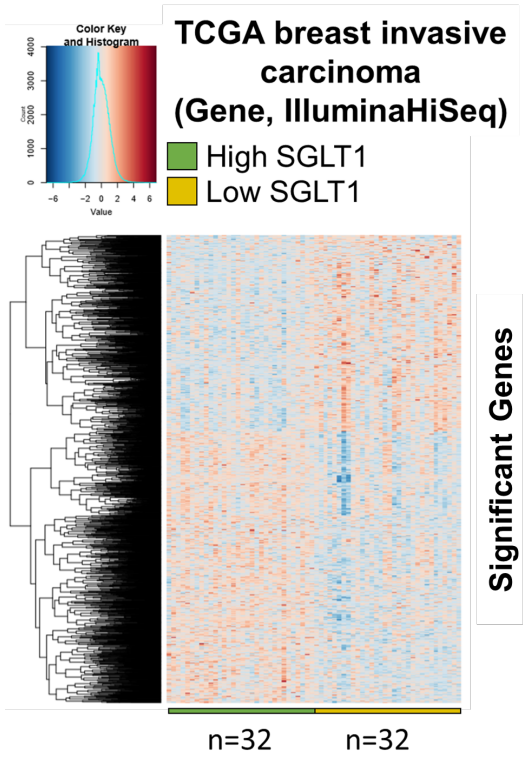
C
Color Key and Histogram
TCGA breast invasive carcinoma (Gene, IlluminaHiSeq)
High SGLT1
Low SGLT1
Significant Genes
n=32
n=32

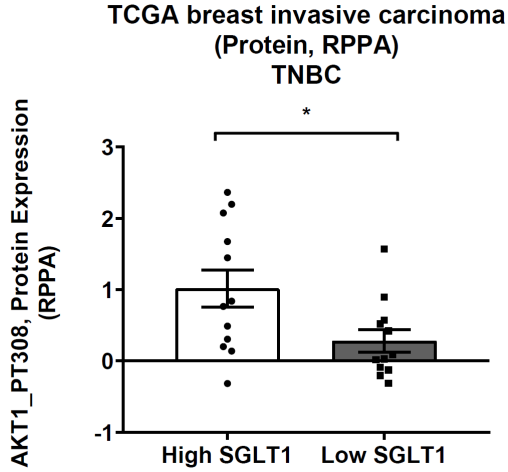
B
TCGA breast invasive carcinoma (Protein, RPPA)
TNBC
*
AKT1_PT308, Protein Expression (RPPA)
High SGLT1
Low SGLT1

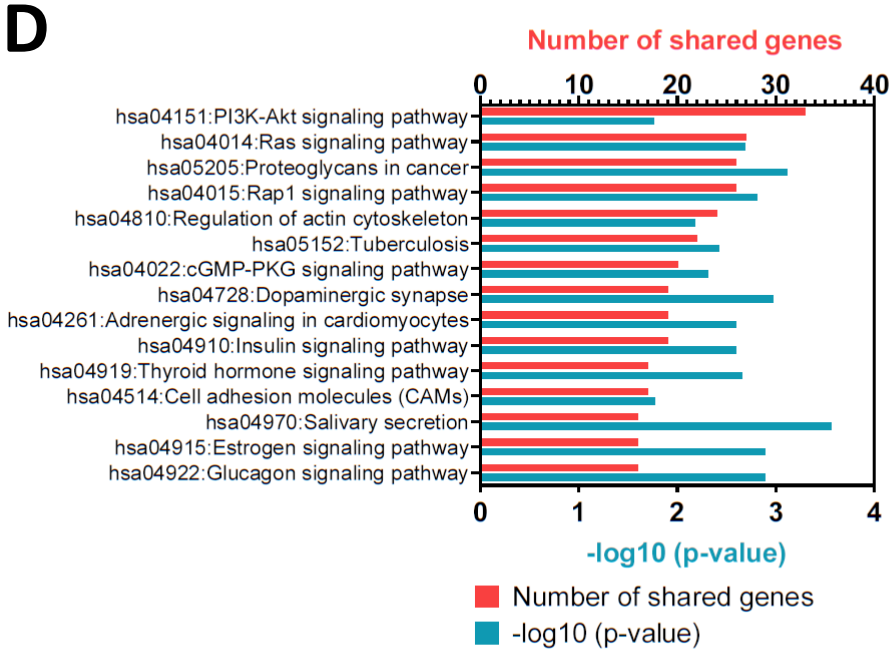
D
Number of shared genes
hsa04151:PI3K-Akt signaling pathway
hsa04014:Ras signaling pathway
hsa05205:Proteoglycans in cancer
hsa04015:Rap1 signaling pathway
hsa04810:Regulation of actin cytoskeleton
hsa05152:Tuberculosis
hsa04022:cGMP-PKG signaling pathway
hsa04728:Dopaminergic synapse
hsa04261:Adrenergic signaling in cardiomyocytes
hsa04910:Insulin signaling pathway
hsa04919:Thyroid hormone signaling pathway
hsa04514:Cell adhesion molecules (CAMs)
hsa04970:Salivary secretion
hsa04915:Estrogen signaling pathway
hsa04922:Glucagon signaling pathway
-log10 (p-value)
Number of shared genes
-log10 (p-value)

Figure 4

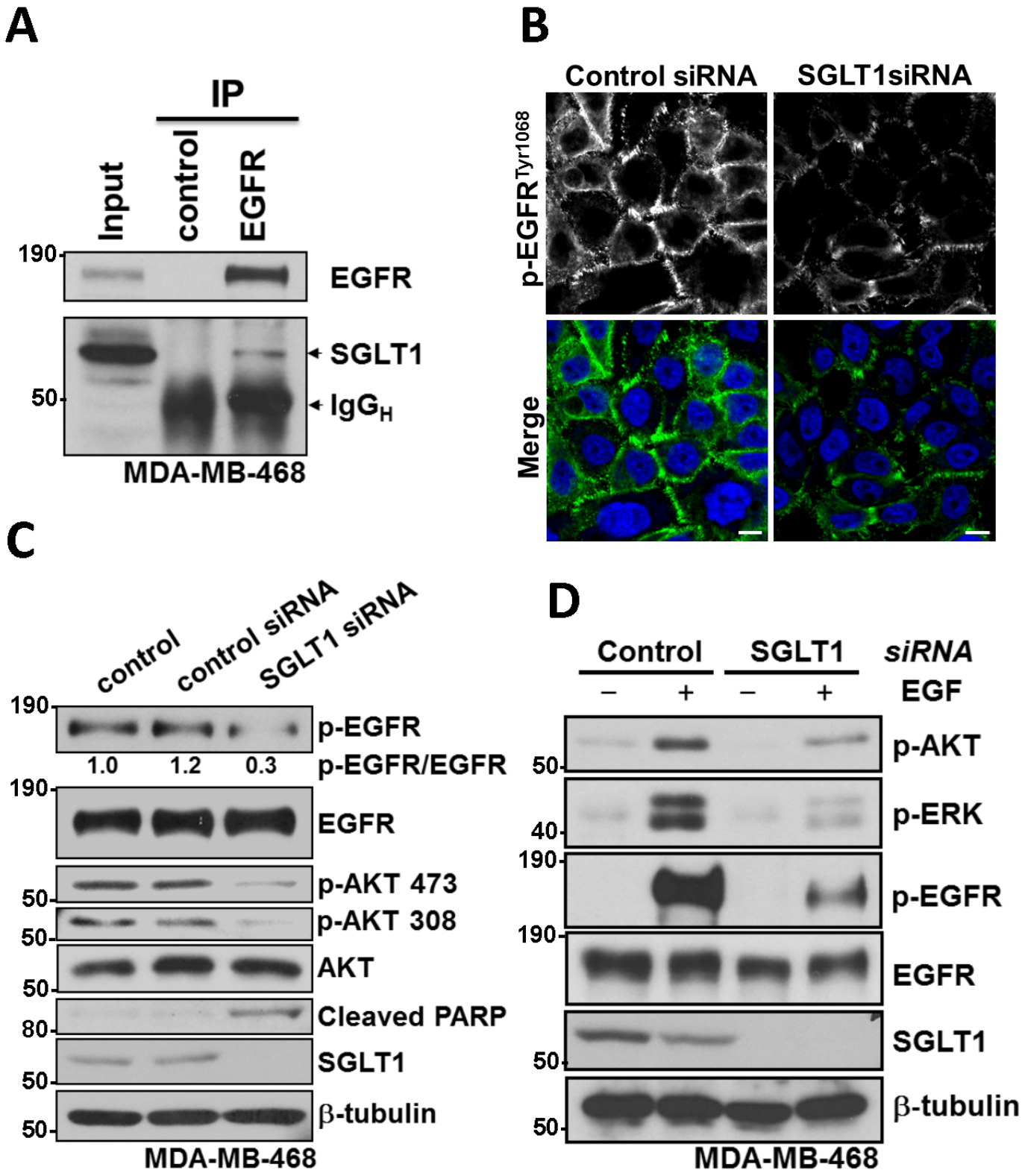
A
IP
Input
control
EGFR
190
EGFR
SGLT1
50
IgG$_H$
MDA-MB-468
B
Control siRNA
SGLT1siRNA
p-EGFR^{Tyr1068}
Merge
C
control
control siRNA
SGLT1 siRNA
190
p-EGFR
1.0
1.2
0.3
p-EGFR/EGFR
190
EGFR
50
p-AKT 473
50
p-AKT 308
50
AKT
80
Cleaved PARP
50
SGLT1
50
β-tubulin
MDA-MB-468
D
Control
SGLT1
siRNA
–
+
–
+
EGF
50
p-AKT
40
p-ERK
190
p-EGFR
190
EGFR
50
SGLT1
50
β-tubulin
MDA-MB-468

Figure 5

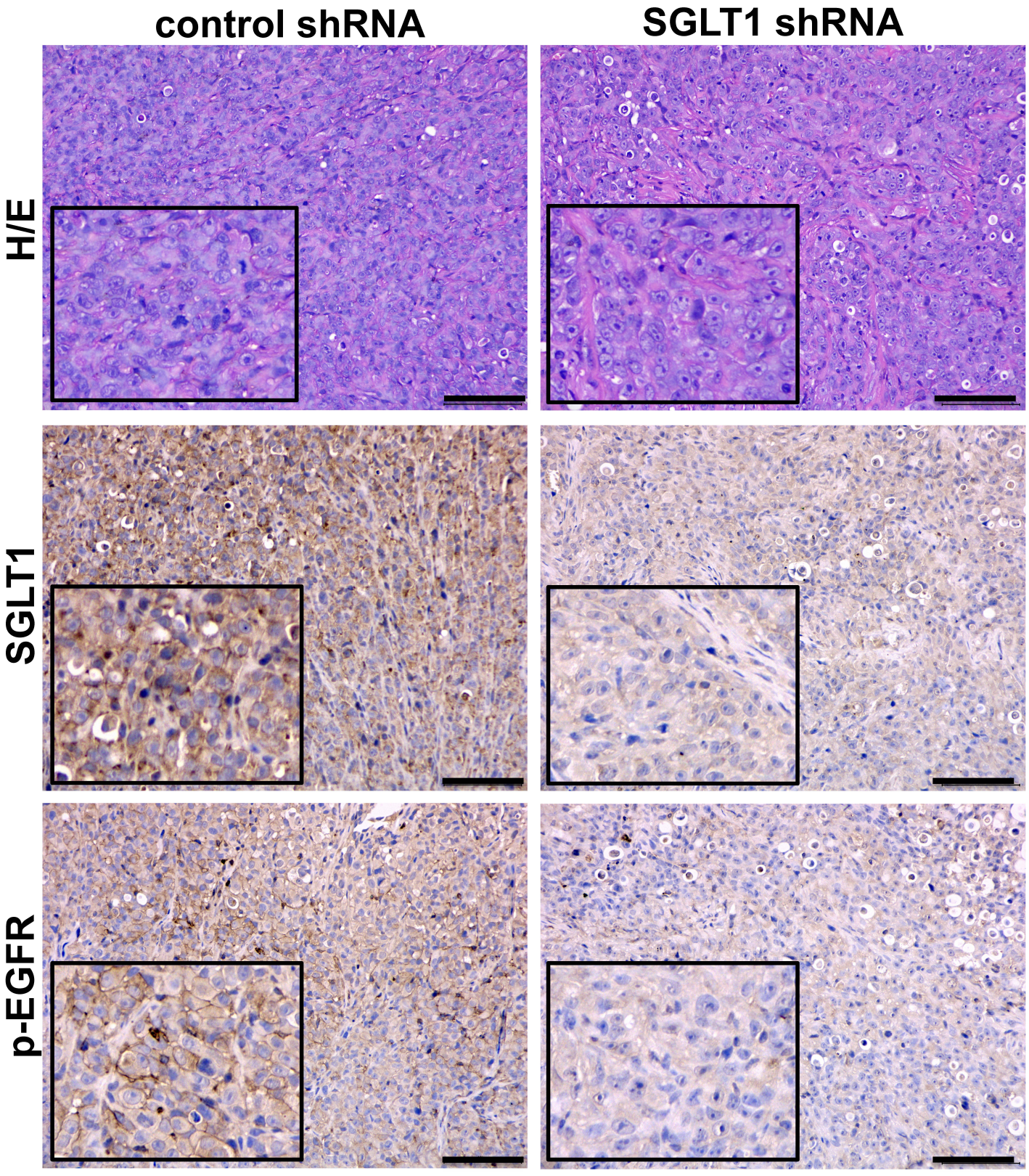

Figure 6

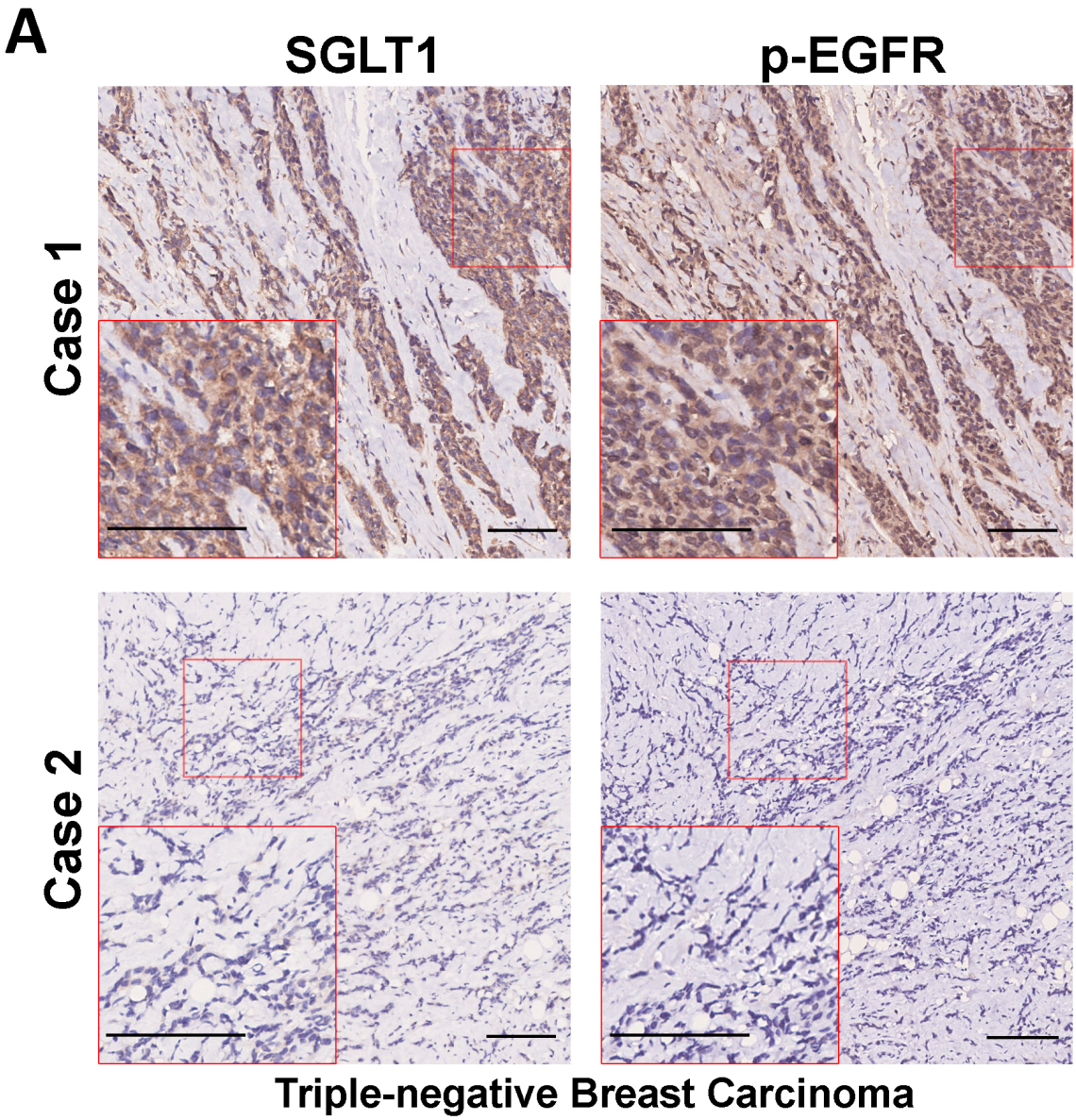
A
SGLT1
p-EGFR
Case 1
Case 2
Triple-negative Breast Carcinoma
B
p-EGFR score
SGLT1 score
0
2
4
6
8
10
12
Pearson:0.41; n=90; P<0.0001

Table 1

Characteristics	N	SGLT1		*P* value
		Low expression	High expression	
Age	90			
≤50	46	28	18	*0.290*
> 50	44	21	23	
Location	90			
Left breast	46	23	23	*0.406*
Right breast	44	26	18	
Grade	90			
I-II	36	19	17	*0.832*
III	54	30	24	
Size	86			
≤2cm	37	26	11	***0.016***
> 2cm	49	21	28	
Positive LN	35			
≤2	21	10	11	*0.728**
> 2	14	5	9	

**P* value of Fisher exact test

The other *P* values were obtained by chi-square test.

SGLT1 is required for the survival of triple negative breast cancer cells via potentiating EGFR activity

Supplementary Figure Legends

Supplementary Figure 1. TCGA analysis of SGLT1 expression levels in different molecular subtypes of breast invasive carcinoma samples (TCGA, Provisional). SGLT1 mRNA expression in four different molecular subtypes of breast cancer. The average of all samples in each molecular subtypes of breast cancers were calculated. Error bars indicate mean ± standard deviation (SD). One-way ANOVA was performed for statistical analysis. ns $P \geq 0.05$; **$P \leq 0.01$; ***$P \leq 0.001$ and ****$P \leq 0.0001$.

Supplementary Figure 2. Knockdown of SGLT1 in TNBC cells via RNAi. Protein expression of SGLT1 in BT549, MDA-MB-436 and MDA-MB-468 cells with the indicated treatments. β-actin was used as a loading control.

Supplementary Figure 3. SGLT1 and its interacting partners. STRING (Search Tool for the Retrieval of Interacting Genes) (https://string-db.org/) analysis showed the interaction between SGLT1 and EGFR.

Supplementary Figure 4. SGLT1 positively regulates EGFR activity. Protein expression of Phospho-EGFR^{Tyr1068}, EGFR and SGLT1 in MDA-MB-468 cells with indicated treatments. β-tubulin was used as a loading control.

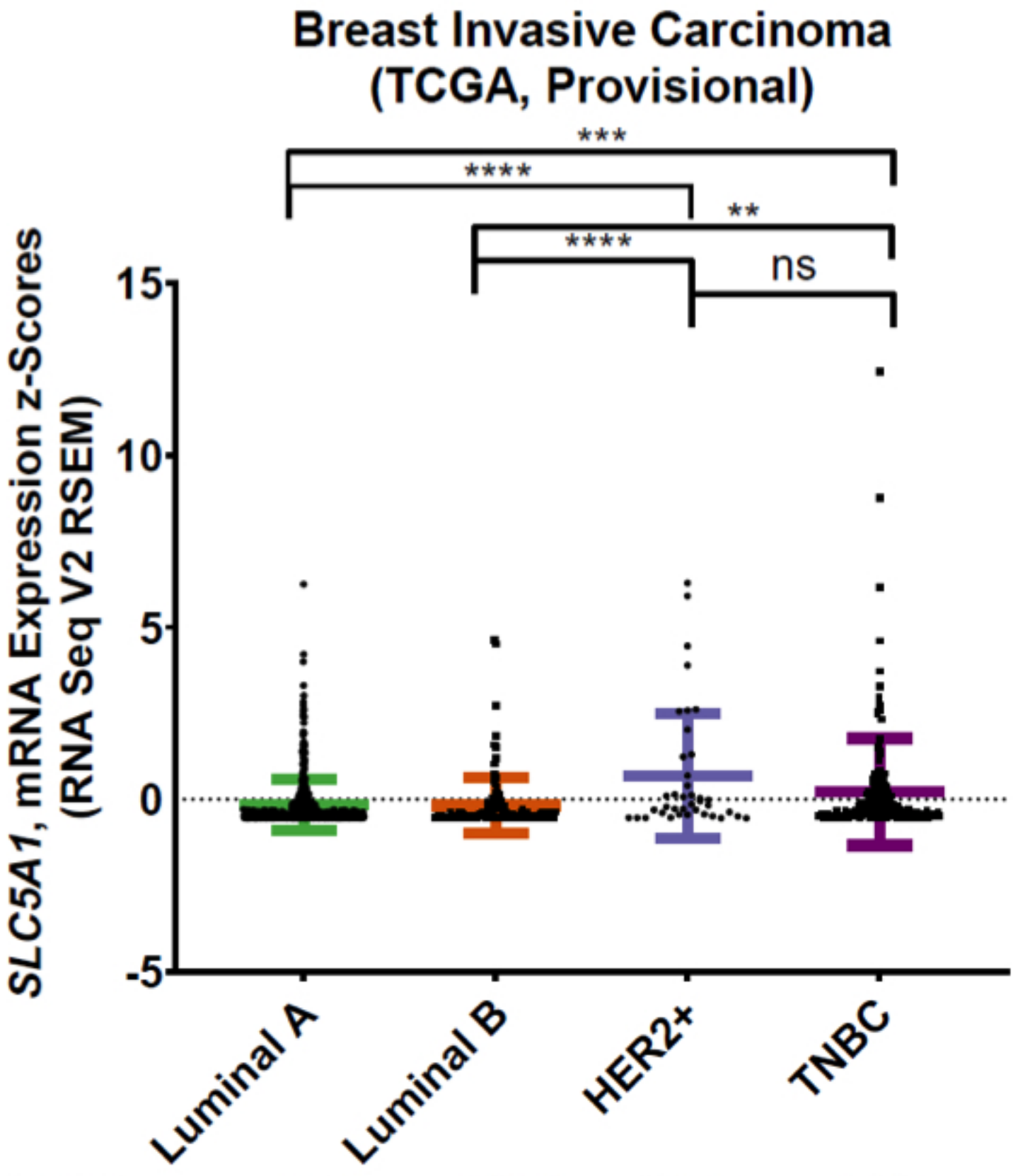
Breast Invasive Carcinoma
(TCGA, Provisional)
***
****
**
****
ns
15
10
5
0
-5
SLC5A1, mRNA Expression z-Scores
(RNA Seq V2 RSEM)
Luminal A
Luminal B
HER2+
TNBC
Mean
-0.16
-0.18
0.68
0.22
Number
505
120
39
160
Molecular subtypes
of breast cancer

Supplementary Figure 2

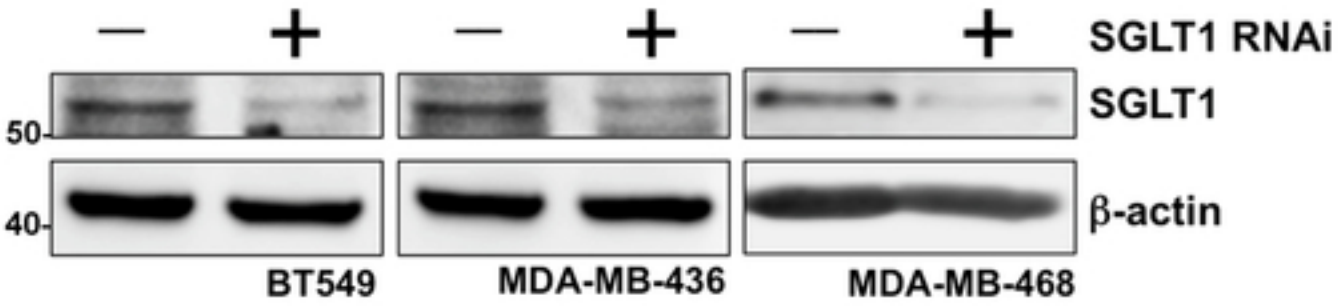

Supplementary Figure 3

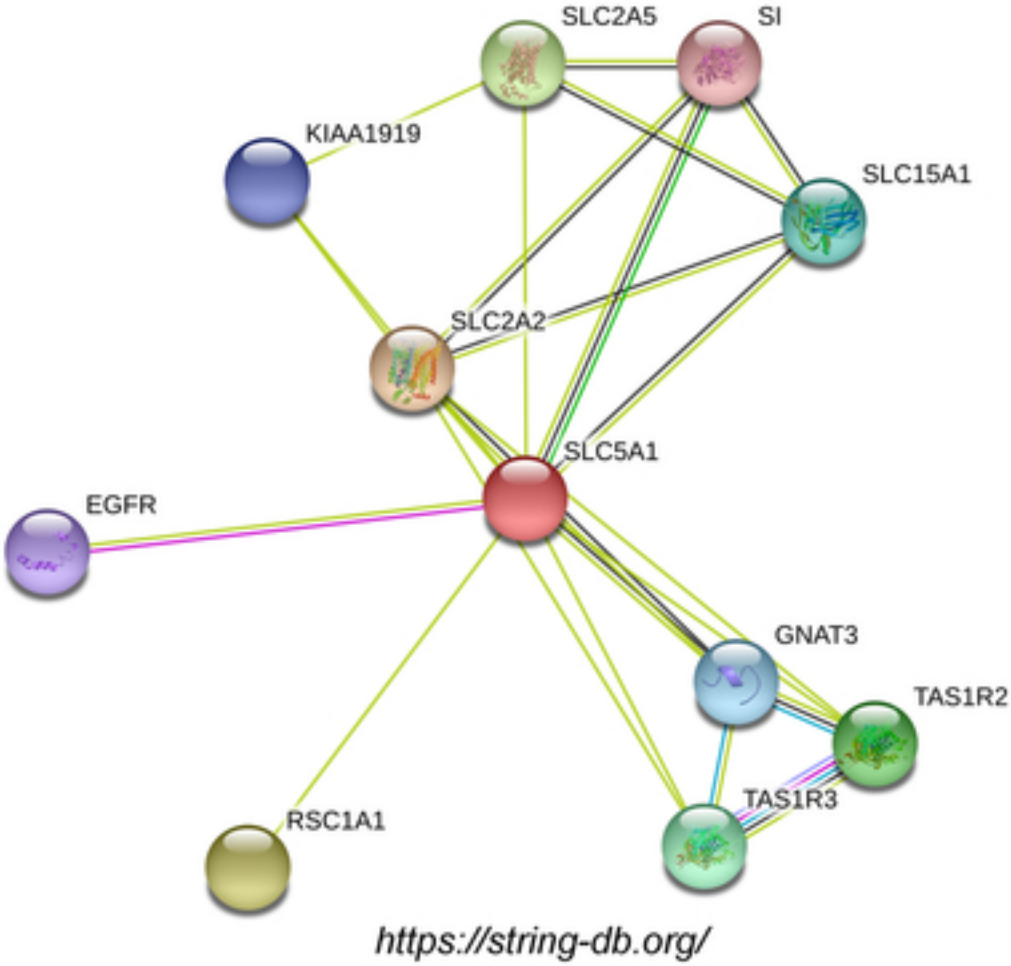

Supplementary Figure 4